Bioluminescent:fluorescent *Trypanosoma cruzi* Reporter Strains as Tools for Exploring Chagas Disease Pathogenesis and Drug Activity

Martin C. Taylor, Alexander I. Ward, Francisco Olmo, Amanda F. Francisco, Shiromani Jayawardhana, Fernanda C. Costa, Michael D. Lewis and John M. Kelly*

Department of Infection Biology,

London School of Hygiene and Tropical Medicine,

Keppel Street,

London WC1E 7HT,

UK.

*corresponding author Email: john.kelly@lshtm.ac.uk

Tel: (+44) (0) 2079272330

Keywords: *Trypanosoma cruzi, in vivo* imaging, bioluminescence, fluorescence, murine models

Abstract

Chagas disease results from infection with the trypanosomatid parasite *Trypanosoma cruzi*. Progress in developing new drugs has been hampered by the long term and complex nature of the condition and by our limited understanding of parasite biology. Technical difficulties in assessing the parasite burden during the chronic stage of infection have also proved to be a particular challenge. In this context, the development of non-invasive, highly sensitive bioluminescence imaging procedures, based on parasites that express a red-shifted luciferase, has greatly enhanced our ability to monitor infections in experimental models. Applications of this methodology have led to new insights into tissue tropism and infection dynamics, and have been a major driver in drug development. The system has been further modified by the generation of parasite reporter lines that express bioluminescent:fluorescent fusion proteins, an advance that has allowed chronic infections in mice to be examined at a cellular level. By exploiting bioluminescence to identify the rare sites of tissue infection, and fluorescence to detect *T. cruzi* at the level of individual host cells in histological sections, it has been possible to investigate the replication and differentiation status of parasites *in vivo* and to examine the cellular environment of infection foci. In combination, these data are providing a framework for the detailed dissection of disease pathogenesis and drug activity.

Introduction

The insect-transmitted protozoan parasite *Trypanosoma cruzi* can invade and replicate in most mammalian cell types. In humans, the infection is characterised by an initial acute stage, which can last 6-8 weeks. During this period, parasites are widely disseminated in organs and tissues, and readily detectable in the bloodstream. The infection then transitions to a chronic phase that can lead to serious pathology, including cardiomyopathy and/or digestive tract megasyndromes, although typically, symptoms take many years to develop. The drugs currently used to treat *T. cruzi* infections, benznidazole and nifurtimox, can have toxic side effects, are non-curative in a significant number of cases [1, 2], and both require to be activated within trypanosomes by the same mitochondrial-localised nitroreductase (TcNTR-1) [3, 4]. Parasites are difficult to detect during the long asymptomatic chronic stage, and their specific location(s) are not well defined. As a result, it is unclear why infections can have such severe consequences, and why only a minority of individuals develop pathology (about one-third of those infected). In addition, difficulties in routinely monitoring the parasite burden has significantly complicated the design and assessment of clinical trials to test new drugs or treatment regimens.

Research on Chagas disease in humans is confounded by the decades long timescale associated with pathology, the diversity of symptomatic outcomes, and the lack of accurate methodology to assess parasitological cure. Consequently, experiments using predictive experimental models have taken on a central role in research, ranging from studies on disease pathogenesis to drug development. Here, we outline recent progress in optimising highly sensitive imaging procedures applicable to murine

models of Chagas disease. These approaches, which are based on parasite strains that express bioluminescent:fluorescent chimeric reporters, represent a valuable addition to the tools available for research on this debilitating infection.

Monitoring murine *T. cruzi* infections using red-shifted bioluminescence reporters

In vivo bioluminescence imaging is a widely used procedure in infectious disease research [5-8]. As a pre-requisite, it requires genetic modification of the corresponding pathogen to express a light-emitting enzyme, such as firefly luciferase. In the presence of molecular oxygen and ATP, this enzyme catalyses the reduction of luciferin resulting in the emission of yellow-green light (wavelength ~560 nm). Bioluminescence imaging of infected mice can then be used to generate a whole-body heat map that allows the location and relative burden of the pathogen load to be inferred (Figure 1A, as example). Despite being a major step forward, the sensitivity of the procedure, when wild-type firefly luciferase is used as the reporter protein, is limited by constraints on the tissue penetration of visible light at wavelengths of less than 600 nm. There are two major factors that cause this, light scattering and absorbance. Rayleigh scattering is greater at shorter wavelengths than at longer wavelengths, and haemoglobin is the major chromophore in tissue, and responsible for the absorbance of non-red light. To mitigate these issues, genetically modified red-shifted luciferases have been engineered to emit light at 617 nm [9], and targeted to the ribosomal locus of *T. cruzi* to ensure stable, high-level expression [10]. In combination, these manipulations have allowed chronic parasite infections to be monitored with unprecedented sensitivity, for periods of more than a year, with a limit of detection close to 100 parasites [11, 12].

In addition to numerous drug screening (Figure 1B) and vaccine assessment applications [13-17], this imaging model has provided several new insights into *T. cruzi* infections. It has been used to demonstrate that chronic infections are highly dynamic, with visible bioluminescence foci appearing and disappearing over a period of hours [11]. It has shown that infections are pantropic during the acute stage, with widespread dissemination throughout the viscera, skeletal muscle and skin. In contrast, during the chronic stage, when the infection burden has been reduced by up to 3 orders of magnitude, it has revealed that parasites are restricted to considerably fewer sites [11]. In BALB/c mice infected with *T. cruzi* CL Brener (TcVI lineage), parasites are located predominantly in reservoir sites in the colon and/or stomach, with infections of other organs and tissues being sporadic (Figure 1C). For example, cardiac infection was observed in only 10% of the mice examined, although infections of the skin and mesentery tissue are more common. This tissue distribution profile is independent of the route of infection (i.p., s.c., i.v. or oral) [11, 17]. Persistent gastro-intestinal (GI) tract localisation of *T. cruzi* was also observed during chronic infections in other mouse:parasite strain combinations, although in some mouse models, parasites were also more widely disseminated [12]. For example, in C3H mice infected with the JR strain of *T. cruzi* (TcI lineage), parasites are more frequently detected in skeletal muscle and the heart, although the level and extent of infection is low compared to the acute stage. Bioluminescence imaging has been used to show that parasite tropism during chronic stage murine infections is controlled by the effectiveness, or otherwise, of tissue-specific immune responses. Immunosuppression of infected mice with cyclophosphamide promotes the expansion of parasites within the GI niche (mainly the stomach and proximal region of the colon) over the first 6-9 days of treatment [12].

This is then followed by widespread dissemination of the infection to other organs and tissues, to produce an infection profile more similar to that in the acute stage, when the adaptive immune response has yet to be induced.

In mice with chronic Chagas disease, heart pathology can develop in the absence of persistent cardiac infection [11]. It has also been observed that higher levels of cardiac fibrosis occur in mouse strains where parasites have a wider tissue distribution during the chronic stage [12, 18]. These findings suggested a model that might explain chagasic pathology, in which periodic trafficking of parasites, or parasite infected cells, from immune-tolerant reservoirs, could lead to recurrent low-level infections at other sites. In organs such as the heart, these intermittent infection foci would initiate a rapid inflammatory immune response targeted at *T. cruzi* infected cells. The cumulative effects of these continuous rounds of local re-infection and parasite elimination over long periods could then lead to collateral tissue damage and fibrosis [19, 20]. This hypothesis has raised a number of questions, the answers to which are central to a fuller understanding of Chagas disease pathogenesis. For example, what is the immunological context of persistent infection foci during the asymptomatic chronic stage? What are the determining factors that allow some tissue sites to act as long-term reservoirs of infection? Does parasite dormancy [21] have a role in immune evasion and/or reduced drug sensitivity? Investigating these and other questions related to disease pathology has been limited by technical challenges in locating, imaging and assessing infection foci at a cellular level during the chronic stage. Below, we describe how modification of the bioluminescence imaging procedures has overcome some of these issues.

Combining bioluminescence and fluorescence allows the routine detection of intracellular parasites in infected mice

As outlined above, bioluminescence imaging can be exploited to monitor *T. cruzi* infections in experimental animal models, and can be adapted to assess the tissue and organ distribution of parasites at different stages of the disease, and to assess drug efficacy (Figure 1B). However, because light emission requires ATP and luciferin, bioluminescence imaging cannot be applied to histological sections, a crucial method for studying *in vivo* host:parasite interactions at a cellular level. Furthermore, during the chronic stage, the parasite burden is so low, that even with bioluminescence-guided excision, it is extremely difficult to detect and image infected cells in tissue sections. One technical advance that has overcome many of these problems is the generation of bioluminescent parasite lines that co-express a fluorescent reporter. This approach is applicable because fluorescence is an intrinsic property of such proteins, and one that survives the processing steps necessary to prepare tissue sections for microscopy. To maintain stable co-expression in these parasites, it was deemed necessary to ensure close linkage of the bioluminescent and fluorescent genes [22], since murine infection experiments can last for up to 18 months, and during this period parasites are not under selective pressure to maintain expression of both reporters. The mNeonGreen protein gene was therefore integrated into the same ribosomal locus as the red-shifted luciferase sequence, to create a fusion gene that expressed a chimeric bioluminescent:fluorescent protein, with the reporters separated by a short linker peptide (Figure 2A). This configuration did not perturb the bioluminescent or fluorescent properties of the expressed protein, and the infectivity of the parasite was unaltered [22]. Bioluminescent tissue foci revealed by *ex vivo* imaging (Figure 2B), can

be excised, fixed, embedded in paraffin, and sections examined by confocal laser scanning microscopy (Figure 2C). Using this approach, it was possible for the first time, to visualise on a regular basis, intracellular parasites in tissue from chronically infected mice. At this stage of the life-cycle, when *T. cruzi* is restricted to a limited number of locations, it was feasible to locate and image infected cells, even when parasite numbers were extremely small, with resolution down to the level of single amastigotes. Furthermore, using antibody co-staining (such as the neuron-specific marker in Figure 2C), it is also feasible to identify the nature of infected cells and to place the infection in its physiological context. A second parasite line has also been generated in which the fluorescent component of the fusion protein was switched to encode an mScarlet sequence [22], opening the way to explore co-infections in fine detail, including *in vivo* drug efficacy.

In the acute stage, as expected from the bioluminescence profile, infections were readily detectable by fluorescence in all tissue types examined, even when host cells contained single amastigotes (Figure 3A). Co-staining with tissue specific markers allows infection foci and their cellular environment to be imaged in detail (Figure 3B). In addition, differentiating intracellular parasites can be visualised *in situ* (Figure 3C), indicating that fusion protein levels in different stages of the life-cycle are sufficient to permit detection. Therefore, bioluminescence:fluorescence imaging provides a framework for investigating the interplay between *T. cruzi* replication and differentiation *in vivo*, and for examining the impact of host cell type, tissue location, disease stage, and drug activity on these processes.

Insights into parasite biology facilitated by bioluminescence:fluorescence imaging

TUNEL assays (terminal deoxynucleotidyl transferase dUTP nick end labelling) [23] and 5-ethynyl-2'-deoxyuridine (EdU) incorporation [24], in combination with the *in vivo* imaging procedures outlined above, provide new approaches for exploring intracellular *T. cruzi* replication and other aspects of infection biology. In trypanosomes, the former can be used to assess mitochondrial DNA (kinetoplast DNA - kDNA) replication [25]. Terminal uridylyl transferase adds fluorescent pyrimidine nucleoside analogues to the transient free 3'-hydroxyl groups that are formed at nicks in newly synthesised strands during replication of the minicircle network. With EdU, replication *in vivo* can be monitored by incorporation of this nucleoside analogue into the parasite nuclear and mitochondrial genomes during DNA synthesis, a process that is detectable by direct fluorescent labelling using copper-catalysed click-chemistry. Both of these approaches have independently demonstrated that parasite replication within individual infected cells is asynchronous *in vivo* [25, 26].

TUNEL positivity in trypanosomes is an early indicator that the cell division process has begun. Initially, kDNA replication can be visualised by staining of the "replication factories" at antipodal sites on each side of the minicircle network (Figure 4A) [22, 26]. Then, as replication of the mitochondrial genome proceeds, the entire disk becomes labelled. Evidence suggests that kDNA replication within individual infected host cells is not co-ordinated at any stage of the disease, or in any organ or tissue type (Figure 4B, as example). Most infected cells contain both labelled and unlabelled amastigotes,

and it was also apparent from these TUNEL studies that amastigotes with replicating kDNA can co-exist in the same host cell as non-dividing trypomastigotes [26].

TUNEL staining of nuclear DNA was not detectable at any stage of parasite replication [26]. The replication status of the parasite genome during murine infections can however be assessed by EdU labelling [25, 26]. Following injection, this nucleoside analogue gets incorporated into the genome of any cell (both host and parasite) in which DNA is undergoing replication during the period of exposure, and is therefore a marker for cells transitioning through S-phase (Figure 5). Judging by the distribution of host cells with labelled nuclei, it can be inferred that EdU is widely available for uptake in mice tissue and that it is stably incorporated [26]. Studies with EdU revealed that replication of nuclear DNA is not synchronised within the parasite population of individual infected cells *in vivo* (Figure 5). Furthermore, as with TUNEL assays, infected host cells were observed that contained both replicating amastigotes and non-replicating trypomastigotes [26]. This lack of developmental synchrony was observed in a wide range of organs and tissues, and during both the acute and chronic stages of the infection (Figure 5A and B). In line with this, imaging has revealed that the number of amastigotes within individual infected cells *in vivo* does not reflect a process that is tightly regulated; parasite numbers are predominantly random, and inconsistent with the type of geometrical progression that would be observed if replication was a co-ordinated event [26]. Recently, it has been reported that when *T. cruzi* intracellular amastigotes are exposed to EdU *in vitro* for 48 hours, there is a growth inhibitory effect [27]. However, this length of exposure is unlikely to be experienced *in vivo* following a single injection (Figure 5); with other thymidine analogues such as bromodeoxyuridine (BrdU), which is also used for DNA labelling experiments, the bioavailability is less

than 15 minutes [28]. Furthermore, in the experiments outlined above, which are based on end-point labelling, EdU incorporation is simply a marker for parasite DNA undergoing replication at the time of exposure.

In addition to the canonical intracellular life-cycle stages of *T. cruzi*, the replicative amastigotes and the flagellated non-dividing trypomastigotes, other parasite forms have been reported *in vitro* [29-33]. However, these had not been observed *in vivo*, their roles during the infection process had not been established, and the possibility that they might represent culture artefacts not excluded. Using the imaging capabilities enabled by the bioluminescent:fluorescent reporter, several non-classical parasite forms have now been detected in mice during both chronic and acute stage infections [26]. Parasites, similar to the sphaeromastigote forms that have been observed *in vitro* [30], were visualised in a range of tissue types (Figure 6). These have an amastigote-like morphology, and possess flagella of varying lengths. Their kinetoplasts are located in the anterior position that is characteristic of replicative forms and they exhibit a variable body length, which has no apparent link to the length of the protruding flagellum. Other types of flagellated parasites, with a morphology more typical of the non-infectious epimastigote forms found in the insect vector, have also been observed *in vivo* [26]. These epimastigote-like forms have an elongated cell body, with the kinetoplast arranged anterior to the nucleus. They have been shown to have wide tissue distribution in mice, and have even been found in the same infected cell as replicating amastigotes and fully differentiated trypomastigotes.

Taken together, these observations suggest that during infection, the *T. cruzi* life-cycle and its regulation are more complex than reported. It is implicit that replication and differentiation are not tightly regulated processes in which all parasites within an infected cell act in unison. Either specific trigger(s) of these developmental events are absent, or alternatively, not all parasites within the intracellular population have the capacity to respond. The identification of non-classical *T. cruzi* forms within infected mice further complicates our ability to understand the mechanisms that underpin parasite growth and differentiation. Whether these forms are developmental intermediates, or have a specific role in propagating the infection, remains unknown. However, their presence widely within the tissues of infected mice could have implications for the drug discovery process. It is unlikely that current high-throughput screening protocols fully capture the sensitivity, or otherwise, of these non-classical forms towards test compounds.

Future prospects

Why do parasites that are present in extremely low numbers during the chronic stage give rise to such severe pathology? Why are infections with *T. cruzi* generally life-long despite a vigorous adaptive immune response? Why are treatment failures such a common outcome of anti-parasitic therapy? Can we develop more effective and safer drugs? Progress in addressing these questions has been particularly hampered by difficulties in detecting and localising parasites during the chronic stage of infection. As outlined in this review, bioluminescence:fluorescence imaging methodology now enables the routine detection of infection foci in predictive experimental models, and provides scope for more detailed examination of the correlation between tissue

tropism and disease pathology. For example, it should now be feasible to visualise the immunological context of parasite infected cells at various stages of the disease, and in a range of tissues and organs, and to explore why parasites are able to avoid immune destruction and persist long-term in specific tissue niches. Similarly, it will be possible to reveal whether treatment failure is associated with an inability to kill parasites in particular tissue locations. The methodology will also be directly applicable to assessing if the recently postulated phenomenon of parasite dormancy [21] has a role in immune evasion and treatment failure. Chronic *T. cruzi* infection is no longer a black-box in which many crucial aspects of parasite biology critical to drug development are hidden from view.

Conflict of Interest: The authors declare no conflict of interest.

Acknowledgements: This work was supported by the following awards. UK Medical Research Council (MRC) Grant MR/R021430/1 to MDL, MRC LID (DTP) Studentship MR/N013638/1 to AW, Fundacion Alfonso Martin Escudero and the Tres Cantos Open Lab Foundation (funded from the People Programme; Marie Curie Actions) grants to FO.

References

[1] Molina I, Gómez i Prat J, Salvador F, Treviño B, Sulleiro E, Serre N, et al. Randomized trial of posaconazole and benznidazole for chronic Chagas disease. N Engl J Med 2014; 370: 1899-1908.

[2] Morillo CA, Marin-Neto JA, Avezum A, Sosa-Estani S, Rassi A Jr, Rosas F, et al. Randomized trial of benznidazole for chronic Chagas' cardiomyopathy. N Engl J Med 2015; 373: 1295-1306.

[3] Wilkinson SR, Taylor MC, Horn D, Kelly JM, Cheeseman, I. A mechanism for cross-resistance to nifurtimox and benznidazole in trypanosomes. Proc Natl Acad Sci USA 2008; 105: 5022-27.

[4] Campos MCO, Leon LL, Taylor MC, Kelly JM. Benznidazole-resistance in *Trypanosoma cruzi*: evidence that distinct mechanisms can act in concert. Molec Biochem Parasitol 2014; 193: 17-9.

[5] Lang T, Goyard S, Lebastard M, Milon G. Bioluminescent *Leishmania* expressing luciferase for rapid and high throughput screening of drugs acting on amastigote harbouring macrophages and for quantitative real-time monitoring of parasitism features in living mice. Cell Microbiol 2005; 7: 383–92.

[6] Hyland KV, Asfaw SH, Olson CL, Daniels MD, Engman DM. Bioluminescent imaging of *Trypanosoma cruzi* infection. Int J Parasitol 2008; 38: 1391–1400.

[7] Myburgh E, Coles JA, Ritchie R, Kennedy PG, McLatchie AP, Rodgers J, et al. *In vivo* imaging of trypanosome-brain interactions and development of a rapid screening test for drugs against CNS stage trypanosomiasis. PLoS Negl Trop Dis 2013; 7: e2384.

[8] Claser C, Malleret B, Peng K, Bakocevic N, Gun SY, Russell B, et al. Rodent *Plasmodium*-infected red blood cells: Imaging their fates and interactions within their hosts. Parasitol Int 2014; 63: 187–94.

[9] Branchini BR, Ablamsky DM, Davis AL, Southworth TL, Butler B, Fan F, et al. Red-emitting luciferases for bioluminescence reporter and imaging applications. Anal Biochem 2010; 396: 290-7.

[10] Lewis MD, Fortes Francisco A, Taylor MC, Kelly JM. A new experimental model for assessing drug efficacy against *Trypanosoma cruzi* infection based on highly sensitive *in vivo* imaging. J Biomolecular Screening 2015; 20: 36-43.

[11] Lewis MD, Fortes Francisco A, Taylor MC, Burrell-Saward H, McLatchie AP, Miles MA, et al. Bioluminescence imaging of chronic *Trypanosoma cruzi* infections reveals tissue-specific parasite dynamics and heart disease in the absence of locally persistent infection. Cell Microbiol 2014; 16: 1285-1300.

[12] Lewis MD, Fortes Francisco A, Taylor MC, Jayawardhana S, Kelly JM. Host and parasite genetics shape a link between *Trypanosoma cruzi* infection dynamics and chronic cardiomyopathy. Cell Microbiol 2016; 18: 1429-43.

[13]. Fortes Francisco A, Lewis MD, Jayawardhana S, Taylor MC, Chatelain E, Kelly JM. The limited ability of posaconazole to cure both acute and chronic *Trypanosoma cruzi* infections revealed by highly sensitive *in vivo* imaging. Antimicrob Agents Chemother 2015; 59: 4653-61.

[14] Francisco AF, Jayawardhana S, Lewis MD, White KL, Shackleford DM, Chen G, et al. Nitroheterocyclic drugs cure experimental *Trypanosoma cruzi* infections more effectively in the chronic stage than in the acute stage. Scientific Reports 2016; 6: 35351.

[15] Brand S, Ko E-J, Viayna Gaza E, Thompson S, Spinks D, Thomas M, et al. Discovery and optimisation of 5-amino-1,2,3-triazole-4-ctarboxamide series against *Trypanosoma cruzi.* J Med Chem 2017; 60: 7284-99.

[16] Calvet CM, Choi JY, Thomas D, Suzuki B, Hirata K, Lostracco-Johnson S, et al. 4-aminopyridyl-based lead compounds targeting CYP51 prevent spontaneous parasite relapse in a chronic model and improve cardiac pathology in an acute model of *Trypanosoma cruzi* infection. PLoS Negl Trop Dis 2017; 11: e0006132.

[17] Mann GS, Francisco AF, Jayawardhana S, Taylor MC, Lewis MD, Olmo F, et al. Drug-cured experimental *Trypanosoma cruzi* infections confer long-lasting and cross-strain protection. PLoS Negl Trop Dis 2020; 14: e0007717.

[18] Lewis MD, Francisco AF, Jayawardhana S, Langston H, Taylor MC, Kelly JM. Imaging the development of chronic Chagas disease after oral transmission. Scientific Reports 2018; 8: 11292.

[19] Lewis MD, Kelly JM. Putting *Trypanosoma cruzi* dynamics at the heart of Chagas disease. Trends Parasitol 2016; 32: 899-911.

[20] Francisco AF, Jayawardhana S, Taylor MC, Lewis MD, Kelly JM. Assessing the effectiveness of curative benznidazole treatment in preventing chronic cardiac pathology in experimental models of Chagas disease. Antimicrob Agents Chemother 2018; 62: e00832-18.

[21] Sanchez-Valdez FJ, Padilla A, Wang W, Orr D, Tarleton RL. Spontaneous dormancy protects *Trypanosoma cruzi* during extended drug exposure. Elife 2018; 2018: 7.

[22] Costa FC, Francisco AF, Jayawardhana S, Calderano SG, Lewis MD, Olmo F, et al. Expanding the toolbox for *Trypanosoma cruzi*: A parasite line incorporating a bioluminescence-fluorescence dual reporter and streamlined CRISPR/Cas9

functionality for rapid *in vivo* localisation and phenotyping. PLoS Negl Trop Dis 2018; 12: e0006388.

[23] Gavrieli Y, Sherman Y, Ben-Sasson SA. Identification of programmed cell death *in situ* via specific labeling of nuclear DNA fragmentation. J Cell Biol 1992; 119: 493-501.

[24] Salic A, Mitchison TJ. A chemical method for fast and sensitive detection of DNA synthesis *in vivo*. Proc Natl Acad Sci USA. 2008; 105: 2415-20.

[25] Taylor MC, Francisco AF, Jayawardhana S, Mann GS, Ward A, Olmo F, et al. Exploiting genetically modified dual-reporter strains to monitor experimental *Trypanosoma cruzi* infections and host:parasite interactions. Methods Molec Biol 2019; 1955: 147-63.

[26] Taylor MC, Ward A, Olmo F, Jayawardhana S, Francisco AF, Lewis MD, et al. Intracellular DNA replication and differentiation of *Trypanosoma cruzi* is asynchronous within individual host cells *in vivo* at all stages of infection. PLoS Negl Trop Dis 2020; 14: e0008007.

[27] Sykes ML, Hilko DH, Kung LI, Poulsen SA, Avery VM. Investigation of pyrimidine nucleoside analogues as chemical probes to assess compound effects on the proliferation of *Trypanosoma cruzi* intracellular parasites. PLoS Negl Trop Dis 2020; 14: e0008068.

[28] Mandyam CD, Harburg GC, Eisch AJ. Determination of key aspects of precursor cell proliferation, cell cycle length and kinetics in the adult mouse subgranular zone. Neuroscience 2007; 146: 108–22.

[29] Almeida-de-Faria M, Freymuller E, Colli W, Alves MJ. *Trypanosoma cruzi*: characterization of an intracellular epimastigote-like form. Exp Parasitol 1999; 92: 263-74.

[30] Tyler KM, Engman DM. The life cycle of *Trypanosoma cruzi* revisited. Int J Parasitol 2001; 31: 472-81.

[31] Kurup SP, Tarleton RL. The *Trypanosoma cruzi* flagellum is discarded via asymmetric cell division following invasion and provides early targets for protective CD8(+) T cells. Cell Host Microbe 2014; 16: 439-49.

[32] Kessler RL, Contreras VT, Marliére NP, Aparecida Guarneri A, Villamizar Silva LH, Mazzarotto GACA, et al. Recently differentiated epimastigotes from *Trypanosoma cruzi* are infective to the mammalian host. Mol Microbiol 2017; 104: 712-36.

[33] Francisco AF, Jayawardhana S, Lewis MD, Taylor MC, Kelly JM. Biological factors that impinge on Chagas disease drug development. Parasitology 2017; 144: 1871-80.

Figure 1. Bioluminescence imaging of chronic murine *T. cruzi* infections. (A) *In vivo* imaging of BALB/c mice infected with *T. cruzi* (CL Brener strain) that express a red-shifted luciferase (ventral images). The number of days post-infection are indicated (left). Following the acute phase, the infection is controlled by the adaptive immune system, but not eradicated. The chronic stage is characterised by highly dynamic bioluminescent infection foci that vary on a day-to-day basis [11]. (B) Mice in the chronic stage of infection (day 106) were treated with 100 mg/kg benznidazole (once daily by the oral route) for 10 days and subjected to regular imaging. Bioluminescence was reduced to background levels by the end of treatment. To promote the outgrowth of any residual parasites, the mice were then immunosuppressed with cyclophosphamide (3 injections of 200 mg/kg i.p., administered at intervals of 3 days) (indicated by red arrow). None of the assessed mice relapsed. (C) *Ex vivo* imaging. Mice, chronically infected with bioluminescent *T. cruzi*, were perfused with d-luciferin in PBS via the heart immediately post-mortem. Organs and tissues were then excised, arrayed in Petri dishes as indicated (bottom right), and incubated in d-luciferin solution during bioluminescence evaluation [11]. Heat-maps are on log10 scales and indicate intensity of bioluminescence from low (blue) to high (red); the minimum and maximum radiances for the pseudo-colour scale are indicated.

Figure 2. Detection of intracellular *T. cruzi* during chronic stage murine infection with parasites expressing a bioluminescent:fluorescent fusion protein. (A) An open reading frame containing linked red-shifted luciferase and mNeonGreen sequences was integrated into a ribosomal locus in *T. cruzi* CL Brener, with the hygromycin resistance gene (*Hyg*) as the selectable marker [22]. The expressed

fusion protein is both bioluminescent and fluorescent. The red-shifted luciferase (*Luc PPyREh*), linker sequence (blue), and mNeonGreen (*mNEON*) components are shown. The ribosomal promoter is indicated by a horizontal arrow. (B) *Ex vivo* imaging of a BALB/c mouse chronically infected (150 days) with parasites expressing the bioluminescent:fluorescent fusion protein. Organs and tissues were arranged as shown in the lower image. Bioluminescent foci can be excised and histological sections prepared [25]. (C) Images of a colon smooth muscle section obtained using the Zeiss LSM 510 confocal microscope. Red, neuron-specific β-tubulin; Blue, DNA stained with DAPI; Green, fluorescent amastigotes.

Figure 3. Fluorescence imaging of intracellular *T. cruzi* in multiple tissue sites during acute stage murine infection. (A) Confocal imaging of spleen and cardiac muscle sections obtained from BALB/c mice in the acute stage of infection (11 days). Red, DNA; Green, fluorescent amastigotes. (B) Oesophageal muscle section derived from a BALB/c mouse in the acute stage of infection (9 days), co-stained with antibodies specific to neuron-specific β-tubulin (purple) and actin (red). Blue, DNA; Green, fluorescent amastigotes. (C) Colon section from a C3H mouse in the acute stage of infection (14 days) showing an infected smooth muscle cell. Blue, DNA; Green, fluorescent trypomastigotes.

Figure 4. The use of TUNEL assays to explore the replicative status of intracellular *T. cruzi in vivo.* (A) Confocal imaging of parasites (CL Brener strain) in tissue sections derived from the colon of a C3H mouse in the acute stage of infection (day 14). Left, parasites indicated by green fluorescence. Right, image showing DNA

(DAPI) and TUNEL staining. Note the staining of antipodal sites on each side of the kDNA minicircle network, indicated by white arrows. Red staining on a green background appears as yellow. (B) Section of smooth muscle from the colon of a C3H mouse in the chronic stage of infection (day 213). Left, image showing DNA (DAPI staining), a single parasite nest (green fluorescence), and TUNEL staining. Note the TUNEL staining of genomic DNA in rapidly dividing gut mucosal cells (white arrow) and the kDNA staining in a minority of *T. cruzi* amastigotes. Right, expansion of a region of the parasite nest (in red circle), with DNA and TUNEL staining highlighting the asynchronous nature of kDNA replication in intracellular *T. cruzi* within an individual infected cell.

Figure 5. The use of EdU labelling and confocal microscopy to explore the replicative status of intracellular *T. cruzi in vivo.* (A) Section of adipose tissue derived from a SCID mouse in the acute stage of infection (day 15) with *T. cruzi* CL Brener, showing parasites (green), DNA (blue) and EdU labelling. The mice were given a single injection with EdU, and sacrificed 16 hours later [26]. DAPI staining allows the large host cell nuclei (indicated by white arrow) to be discriminated from the smaller highly abundant parasite nuclei/kDNA. A minority of host cells were stained with EdU, indicating they were in S-phase during the period of exposure. Within individual infected host cells, parasite staining was intermittent, demonstrating that DNA replication is asynchronous within the population. (B) Sections of colon tissue taken from a C3H mouse during the chronic stage of infection (day 183) showing two infected smooth muscle cells. Asynchronous parasite DNA replication can be inferred from the EdU labelling pattern.

Figure 6. Non-classical morphologies displayed by *T. cruzi* parasites during murine infections revealed by confocal imaging. (A) Section of smooth muscle derived from the rectum of a BALB/c mouse during acute stage infection (day 19) with *T. cruzi* CL Brener strain. Parasites, green; host cell DNA, red (parasite DNA appears as yellow, due to overlap with green fluorescence). (B) Cardiac tissue imaged 19 days post-infection. Some parasites have an amastigote-like morphology, and exhibit variable body and flagellum length, with the kinetoplasts located in an anterior position. Adapted from reference [26]. Bar = 5 μm.

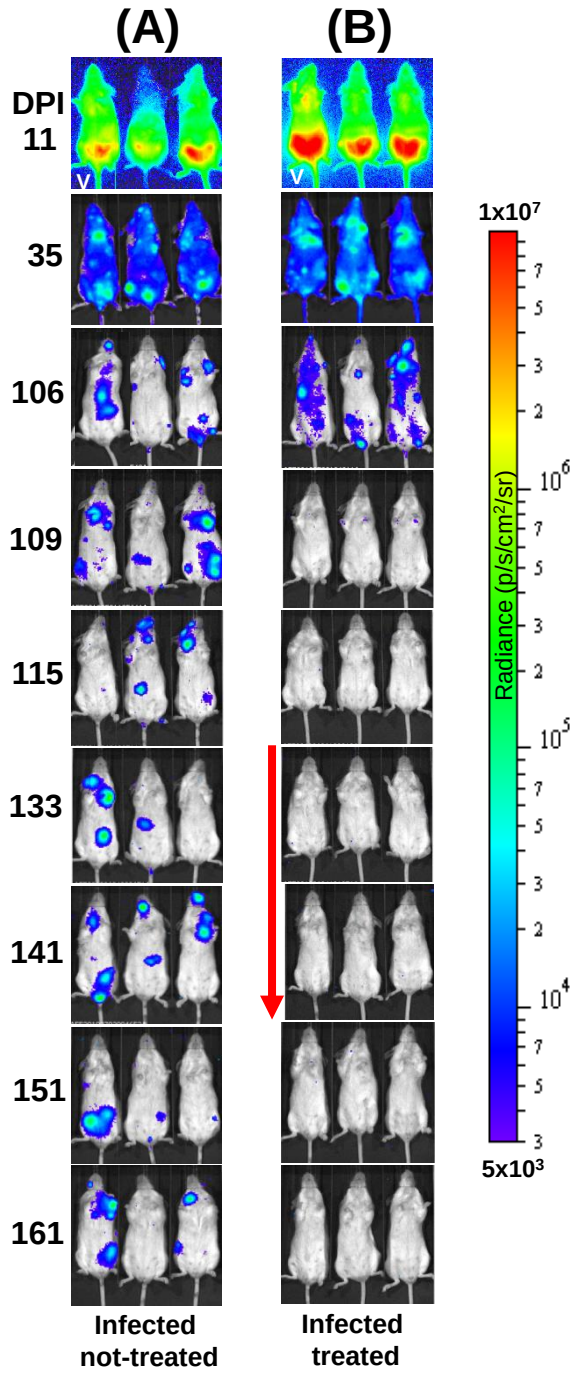
(A)
(B)
DPI
11
35
106
109
115
133
141
151
161
Infected
not-treated
Infected
treated
1x10⁷
Radiance (p/s/cm²/sr)
10⁶
10⁵
10⁴
5x10³

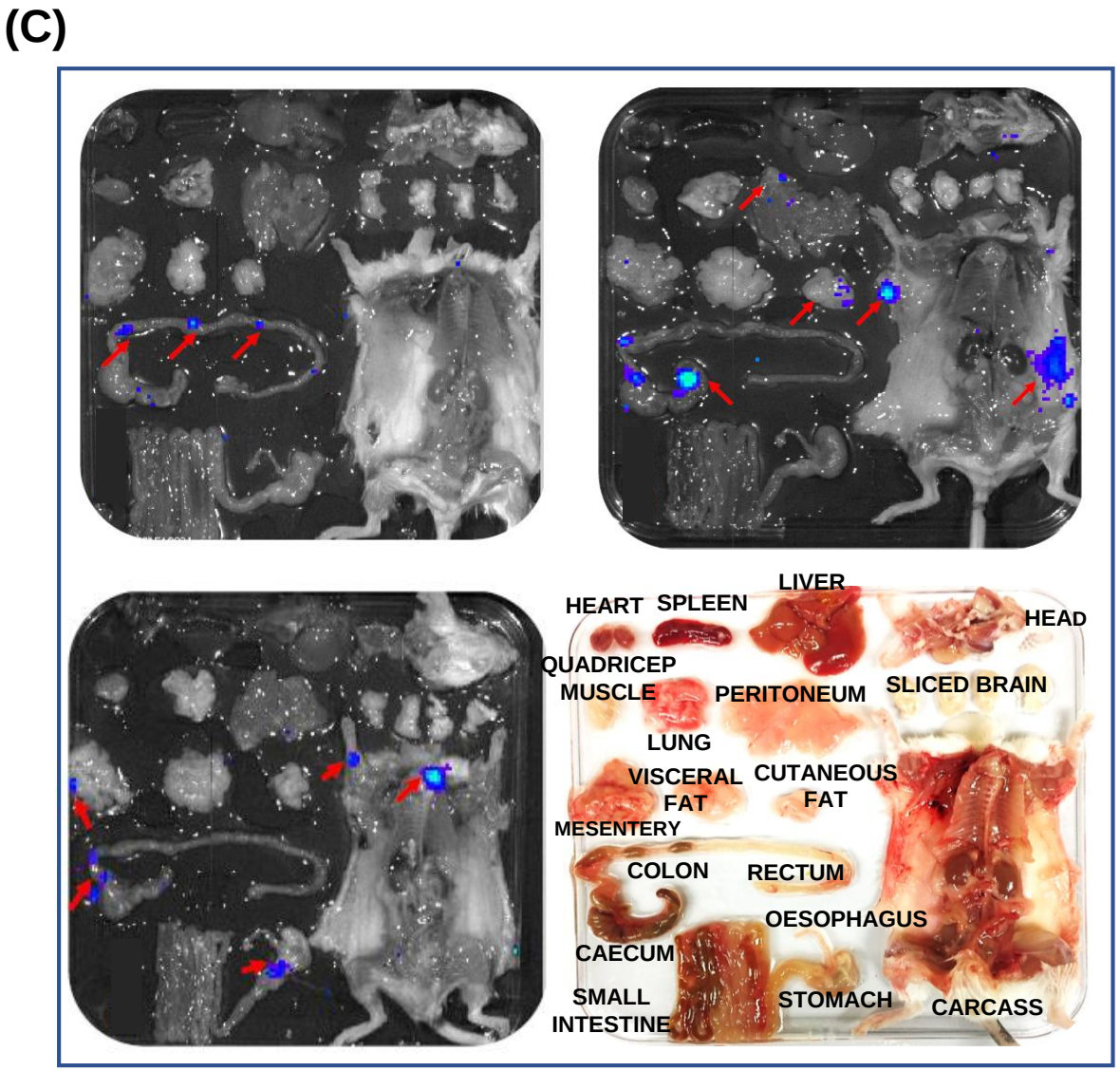
(C)
HEART
SPLEEN
LIVER
HEAD
QUADRICEP
MUSCLE
PERITONEUM
SLICED BRAIN
LUNG
VISCERAL
FAT
CUTANEOUS
FAT
MESENTERY
COLON
RECTUM
OESOPHAGUS
CAECUM
SMALL
INTESTINE
STOMACH
CARCASS

Figure 1

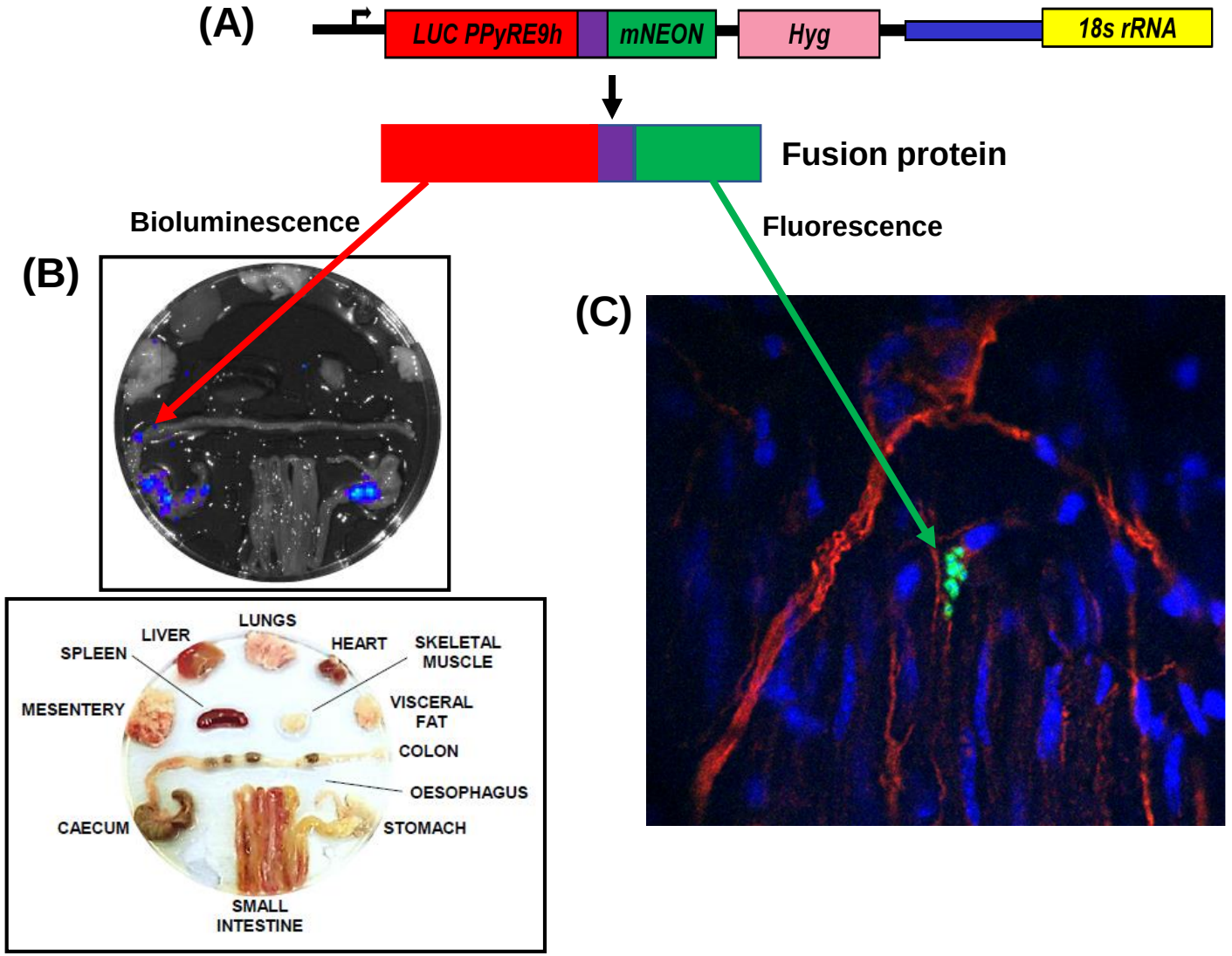
(A)
LUC PPyRE9h
mNEON
Hyg
18s rRNA
Fusion protein
Bioluminescence
Fluorescence
(B)
(C)
LUNGS
LIVER
SPLEEN
HEART
SKELETAL MUSCLE
MESENTERY
VISCERAL FAT
COLON
OESOPHAGUS
CAECUM
STOMACH
SMALL INTESTINE

Figure 2

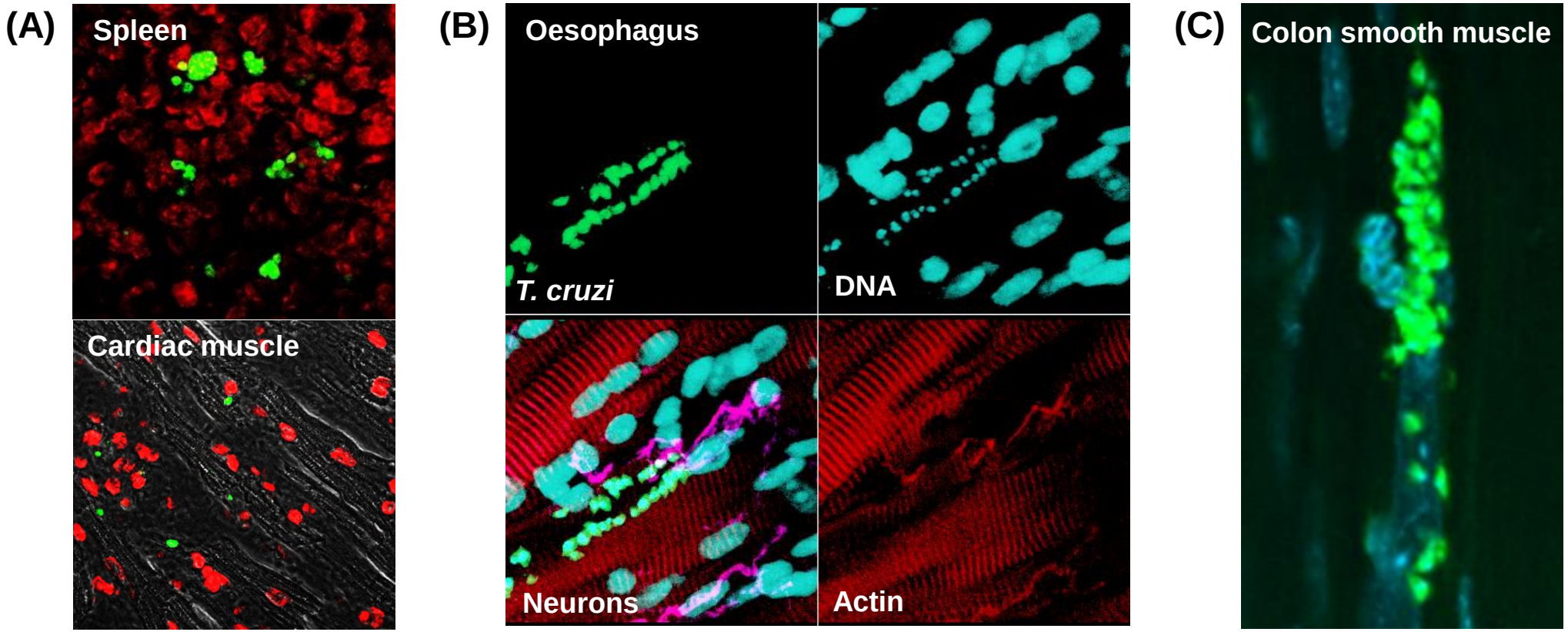
(A)
Spleen
Cardiac muscle
(B)
Oesophagus
T. cruzi
DNA
Neurons
Actin
(C)
Colon smooth muscle

Figure 3

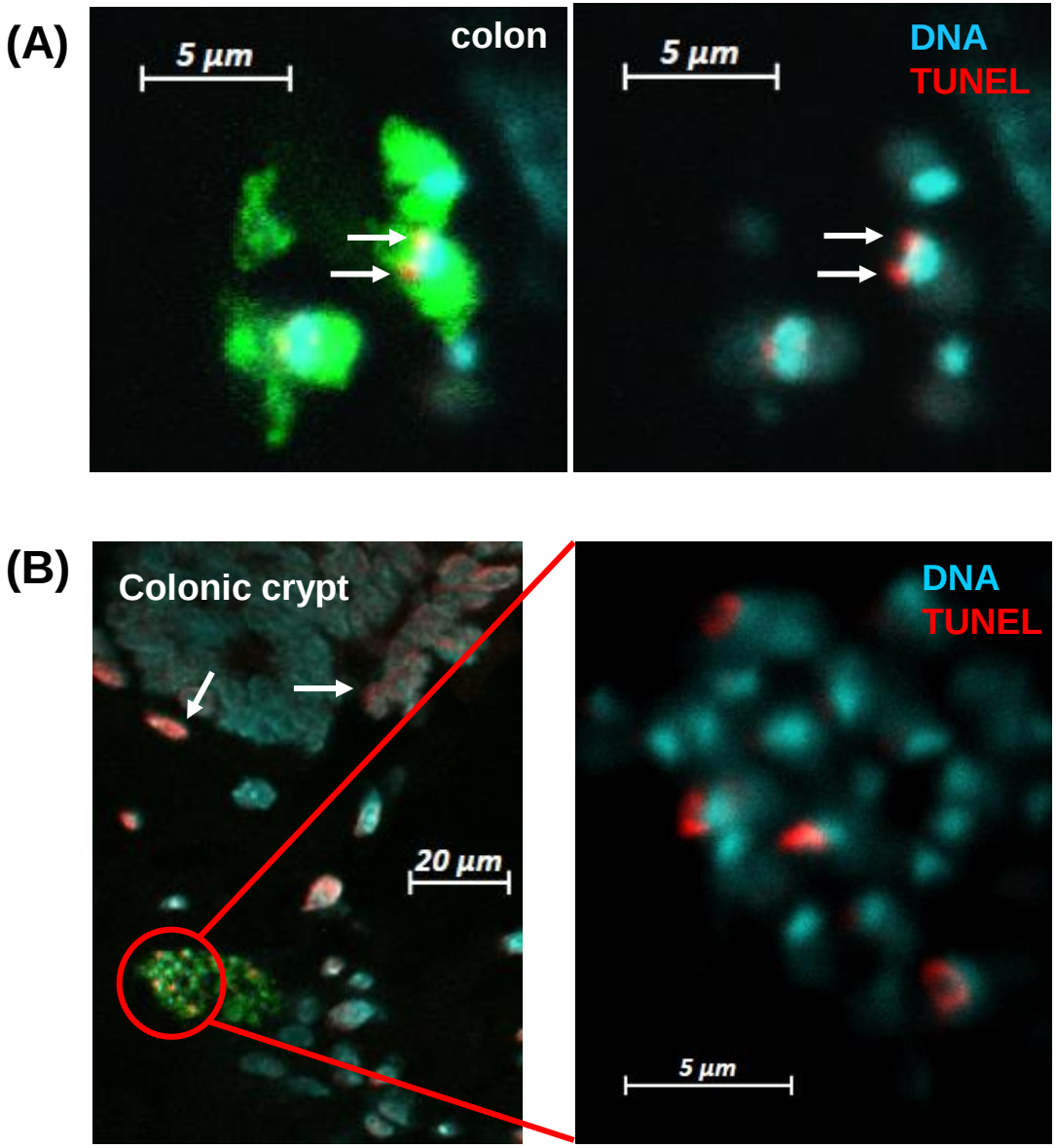

Figure 4

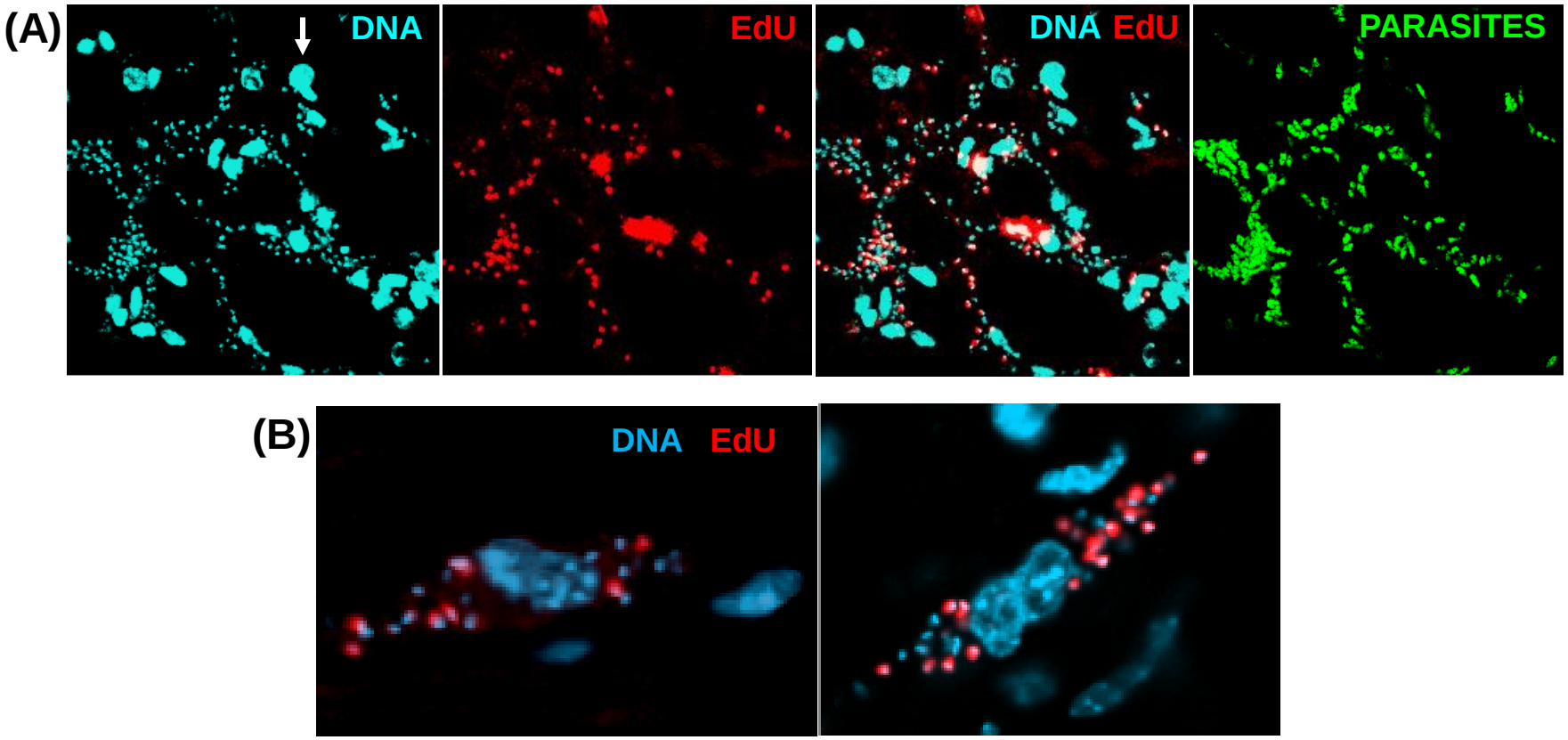

Figure 5

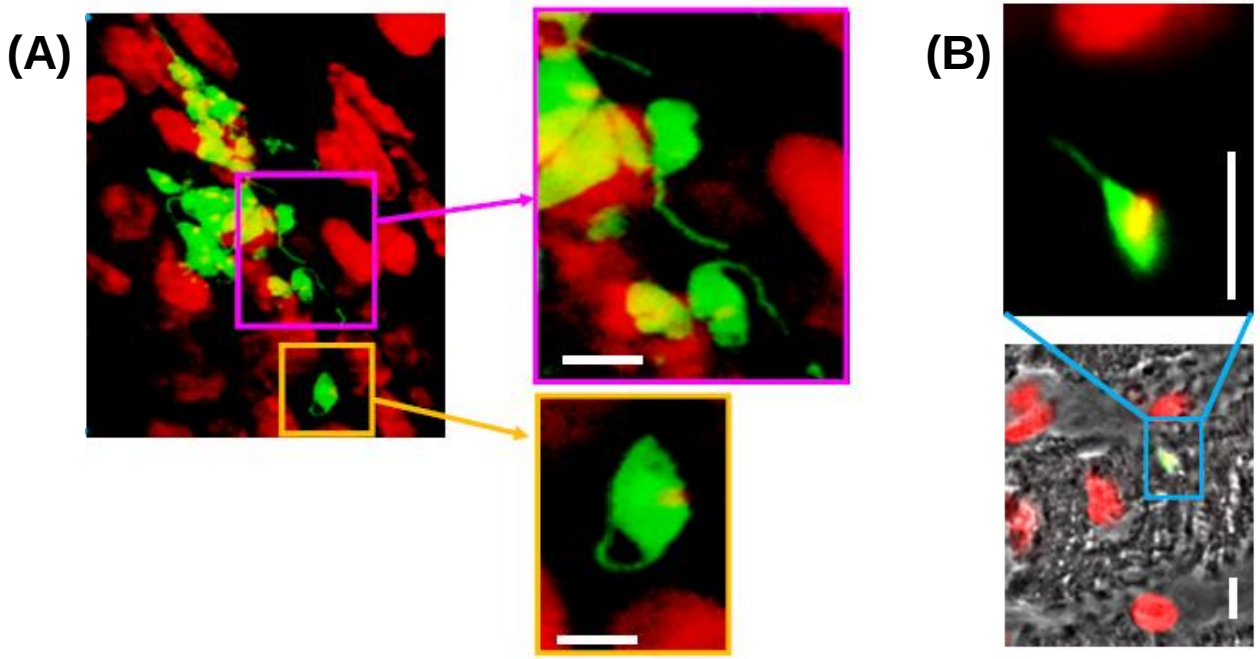

Figure 6